

# Compact dual-band dual-mode circular patch antenna with broadband unidirectional linearly polarised and omnidirectional circularly polarised characteristics

ISSN 1751-8725

Received on 18th April 2015

Revised on 12th August 2015

Accepted on 20th September 2015

doi: 10.1049/iet-map.2015.0266

www.ietdl.org

Wen-Quan Cao ✉

Communications Engineering, PLA University of Science and Technology, Nanjing, Jiangsu, People's Republic of China

✉ E-mail: cao\_wenquan@163.com

**Abstract:** A novel probe-feed single-layer circular patch antenna with dual-band dual-mode dual polarisation is proposed in this study. By using modified mushroom structure, dual-band dual-mode characteristic is realised as former designs. Due to the loading structure including four curved patches added around the circular radiating patch, bandwidth is broadened for the patch mode ( $n=1$  mode) with unidirectional linearly polarised characteristics at the upper frequency band. By loading with four curved branches in the ground plane, circularly polarised property for the dipole mode ( $n=0$  mode) with omnidirectional radiation patterns is achieved at the lower frequency band. Parameter analysis is made to study this antenna and one prototype is fabricated to confirm the property. Moreover, the measured results are obtained with  $-10$  dB impedance bandwidths of 227.5 MHz (5.1% at the centre frequency of 4.42 GHz) and 857.5 MHz (14.9% at the centre frequency of 5.74 GHz), and maximum gain of 1.1 and 7.1 dB for the dipole mode and patch mode, respectively. With the advantages of simple structure, wide bandwidth, radiation pattern selectivity and polarisation diversity, this antenna concept is valuable in wireless communications.

## 1 Introduction

Multifunction has become one of the most valuable merits for the antennas required in the modern wireless communication systems. With the advantages of low profile, easy fabrication and low cost, microstrip antennas have been used to design various antennas to meet the requirement [1]. Among these multifunction microstrip antennas, antenna with dual-band dual-mode dual-polarisation (DBDMDP) property is widely researched in the practical applications. The major disadvantage of the reported DBDMDP antennas is their complex radiating geometry with dual- or multi-layers and feed network with dual- or multi-ports which restricted their applications in some extent [2–9].

With the unusual electromagnetic property, metamaterial structures were good option in designing novel antennas and components recently [10, 11]. By introducing the modified mushroom structures under conventional radiating patch, DBDMDP feature is realised for the probe-fed microstrip antenna [12, 13]. Composite right-/left-handed transmission line (CRLH TL) theory was used to analyse the working principle. Then based on the concept of circularly polarised (CP) characteristic for omnidirectional mode by adopting a metamaterial TL [14, 15], a compact dual-band antenna with both unidirectional LP and omnidirectional CP properties was realised [16]. Due to the curved branches in the radiating patch, the dipole mode owns CP property. Then several metamaterial-based microstrip antennas with multifunction are designed and realised accordingly [17–19]. However, these antennas limited to narrow bandwidth of about 1–3% and complicated structures of two-layer substrates which restrict their applications. Then two schemes including the reconfigurable microstrip antenna and metamaterial-based phase-shifting line antenna were designed to broaden the impedance bandwidth. Nevertheless, they were realised at the expense of complex structure and high cost [20, 21].

To solve the bandwidth problem, a novel compact dual-band planar antenna with dual mode dual polarisation and enhanced bandwidth for each band is proposed in this paper. The dual-band

dual-mode characteristic is realised by using modified metamaterial structure. Bandwidth enhancement is achieved by loading four curved patches around the circular radiating patch. By employing curved branches in the ground plane, CP property for the  $n=0$  mode with omnidirectional radiation patterns is obtained. To confirm the antenna property, one antenna prototype is fabricated and measured. Measured results of the probe-feed single-layer antenna show that  $-10$  dB impedance bandwidths are 227.5 MHz (5.1% at the centre frequency of 4.42 GHz) and 857.5 MHz (14.9% at the centre frequency of 5.74 GHz), and the maximum gains are 1.1 and 7.1 dB for the dipole mode and patch mode, respectively. Here, the antenna is designed using the finite element method-based high frequency structure simulator (HFSS) software.

## 2 Antenna analysis and design

The schematic diagram of the proposed antenna is described in Fig. 1. The antenna consists of only one substrate layer. On the top surface, a slotted circular radiating patch with four curved patches around which can be considered as parasitical patches is printed on a circular substrate with radius of  $R_4$ , height of  $h$  and dielectric constant of  $\epsilon_r=2.2$ . On the bottom surface, the ground plane with size of  $R_5$  is loaded with four curved branches around the circumference of the substrate.

The slotted circular radiating patch with size of  $R_1$  can be regarded as metamaterial cells made up of four modified mushroom structure units. So the circular patch antenna can be treated as distributed periodic structure and analysed by the similar CRLH TL theory. The mushroom vias on the edge of the circular patch provide the shunt inductance (also named left-handed inductance) and the strip slots give the series capacitance (also named left-handed capacitance) as discussed in the former work [12, 13]. Thus the multi-frequency dual-mode property can be excited by the inner mushroom structure. In this work, we investigate the property of the  $n=0, +1$  modes. Two major factors, including the distance

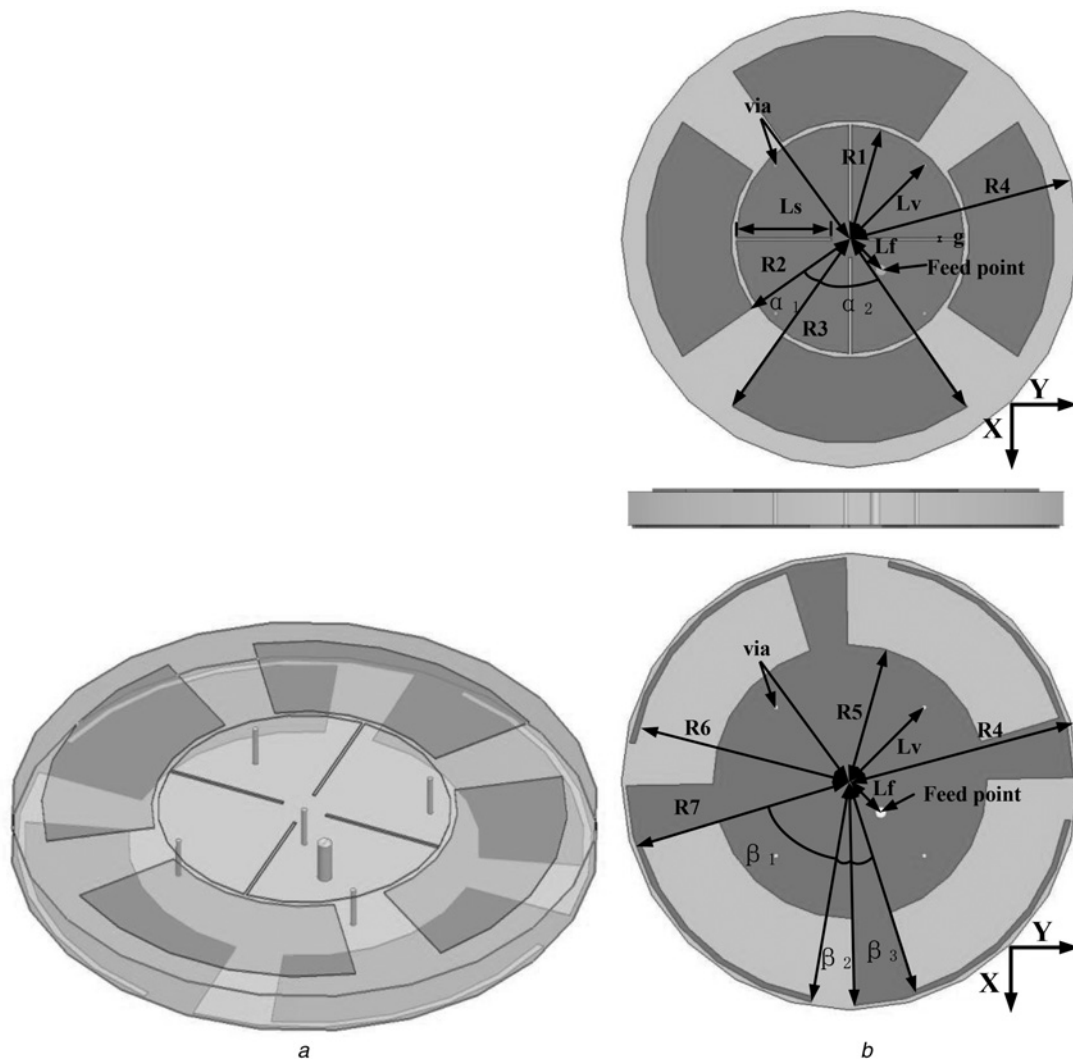


**Fig. 1** Schematic diagram of the compact antenna  
*a* 3D view  
*b* Top view, side view and bottom view (from up to down)

$L_f$  from the centre of the radiating patch to the location of the feed probe and the geometry of the centre via, can be used to tune the impedance match.

As the theory analysis of the meta-based antennas has been proposed in former manuscripts [8–12], we will not discuss working modes of this antenna in detail but pay attention to the far

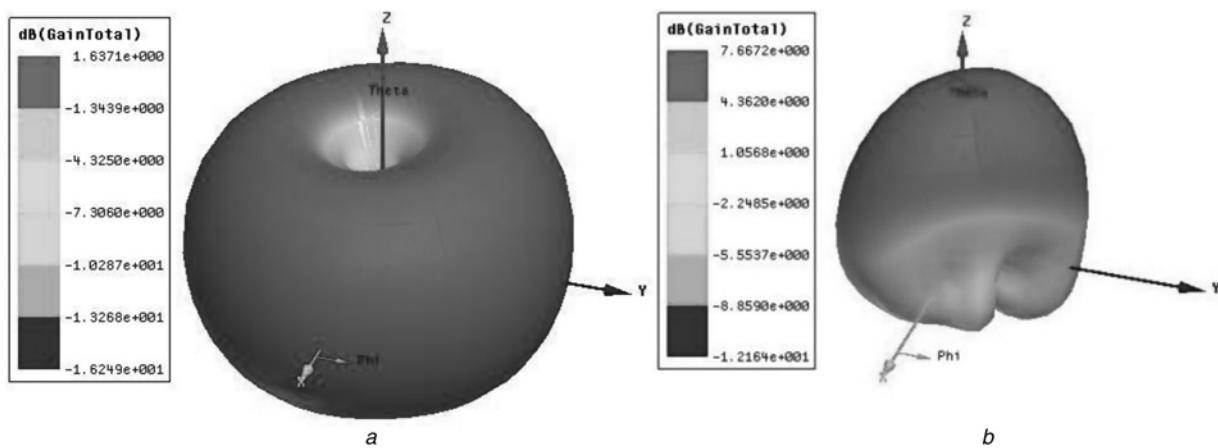


**Fig. 2** Simulated radiation patterns  
*a*  $n=0$  mode at 4.51 GHz  
*b*  $n=1$  mode at 5.8 GHz

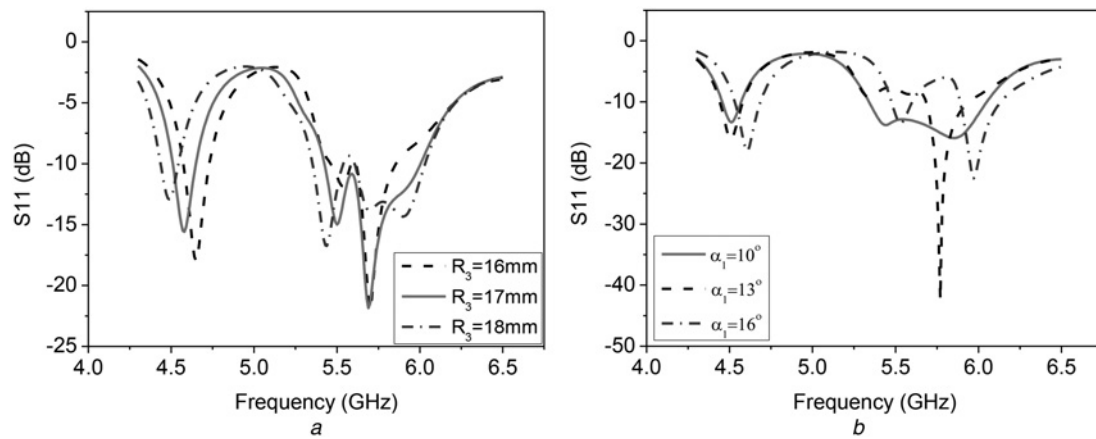


**Fig. 3** Simulated  $S_{11}$  against frequency for the proposed antenna with various parasitical patch size ( $R_3$ ) or gap size ( $\alpha_1$ ), other parameters are the same as listed in Table 1

**Table 1** Parameters of the proposed DBDMDP antenna

$R_1$	$R_2$	$R_3$	$R_4$	$R_5$	$R_6$	$R_7$	$R_{pin}$	$g$
10	10.4	17.9	20	12	19.1	19.6	0.2	0.2
mm	mm	mm	mm	mm	mm	mm	mm	mm
$L_v$	$L_s$	$L_f$	$\alpha_1$	$\alpha_2$	$\beta_1$	$\beta_2$	$\beta_3$	$h$
9.2	8.4	3.8	10°	80°	63°	11°	16°	3
mm	mm	mm						mm

field radiation patterns of the two modes in this work. For the dipole mode, the electric-field distribution in-phase with the equivalent magnetic vector forms a magnetic loop along the radiating patch edges. Therefore, omnidirectional radiation patterns can be realised,

which is confirmed at 4.51 GHz for the  $n=0$  mode and is shown in Fig. 2a. As shown in Fig. 2b, for the  $n=+1$  mode at 5.8 GHz, the electric field is out-of-phase corresponding to a half wavelength along the feeding line ( $\varphi=45^\circ$ ), thus directional radiation pattern similar to a patch antenna can be obtained. The simulated radiation patterns for the two modes confirm the prediction.

Since four curved patches considered as parasitical patches are added along the radiating patch circumference, new resonant points can be introduced and wide impedance bandwidth can be obtained by merging different resonant points together. Fig. 3 describes the simulated  $S_{11}$  against frequency for the proposed antenna with various parasitical patch size ( $R_3$ ) or gap size  $\alpha_1$ , other parameters are the same as listed in Table 1. It can be found

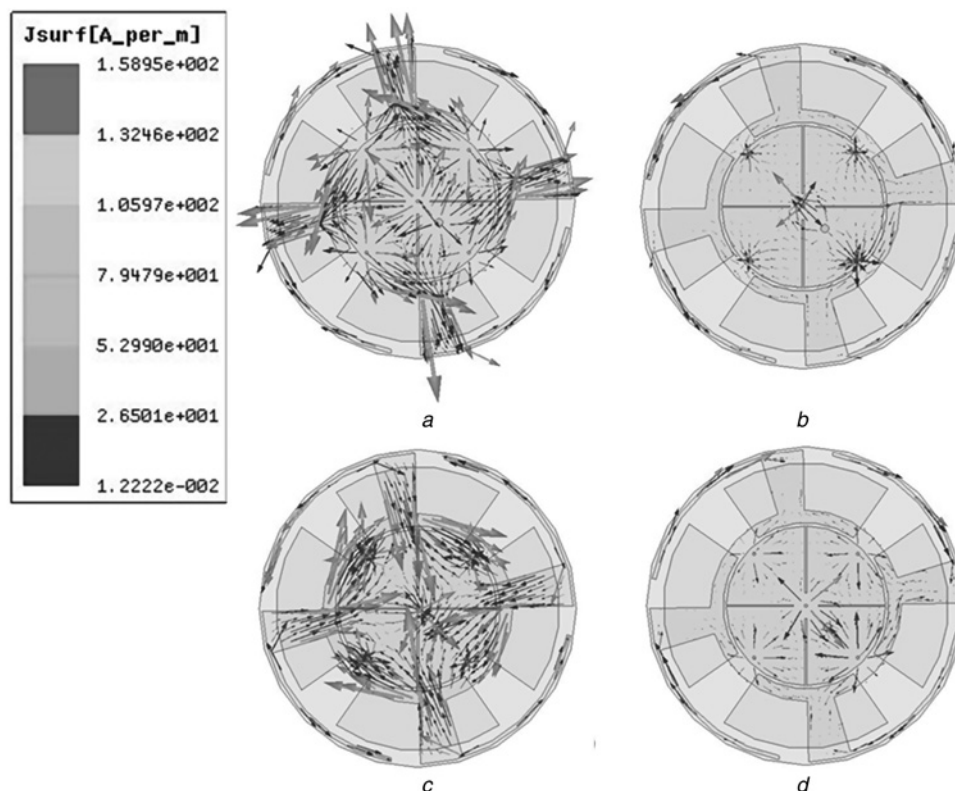


**Fig. 4** Surface current distribution of the proposed antenna for the  $n=0$  mode

a  $t=0$   
 b  $t=T/4$   
 c  $t=T/2$   
 d  $t=3T/4$

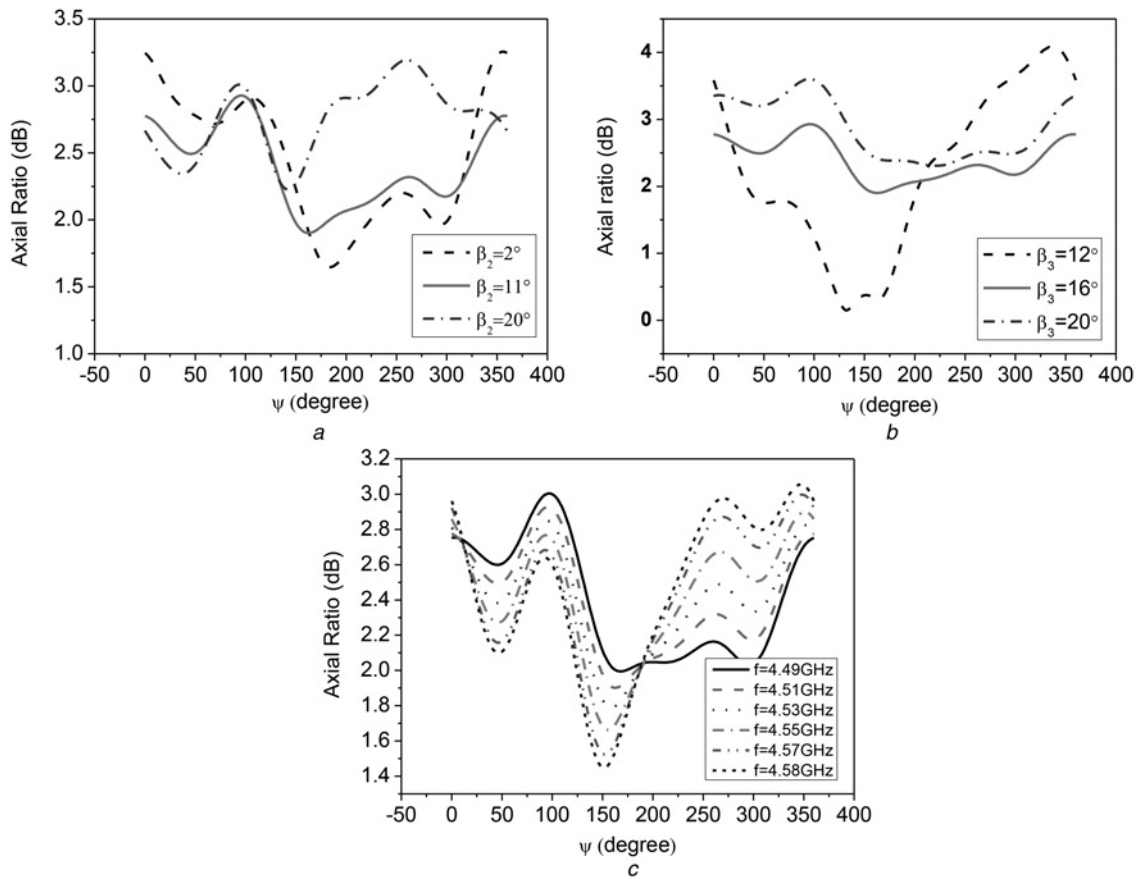


**Fig. 5** Simulated AR for the proposed antenna with various parameters

a  $\beta_2$   
 b  $\beta_3$   
 c Frequencies, other parameters are the same as listed in Table 1

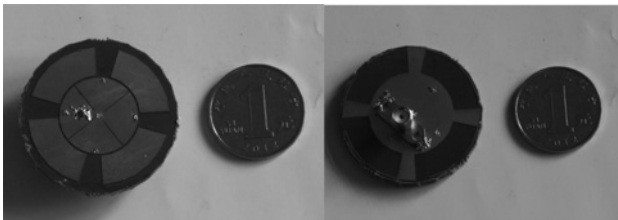


**Fig. 6** Photographs of the proposed antenna. left: top view; right: bottom view

that new resonant points can be introduced by using longer patches in the radial direction. Broad bandwidth is achieved by merging these resonant points together, which is shown in Fig. 3a. Fig. 3b shows that the gap size between each parasitical patch is a vital factor determining the coupling capacitance, thus the impedance matching of the  $n = 1$  mode can be optimised by tuning the gap angle  $\alpha_1$ . It can also be found that minor influence exists on the  $n = 0$  mode by changing the parasitical patch geometry.

Unlike the designs in [16, 18], four curved branches are employed in the ground plane instead of the radiating patch in this work. Since modification of the ground geometry does not affect the radiation

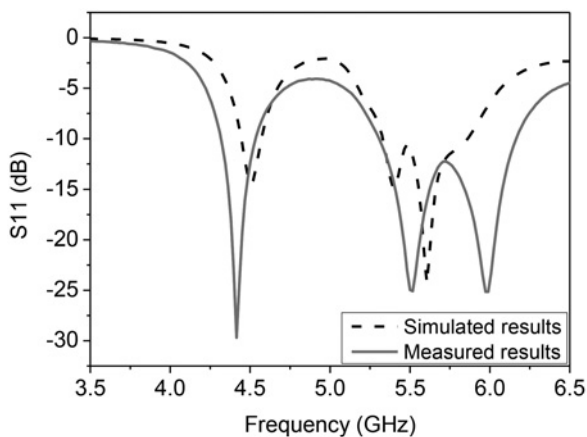


**Fig. 7** Simulated and measured reflection coefficients of the proposed antenna

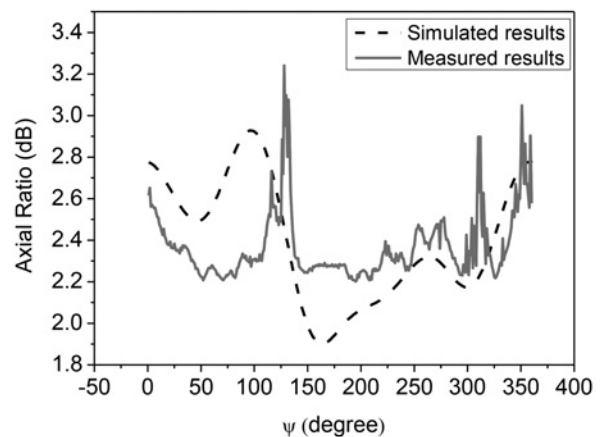


**Fig. 8** Simulated and measured axial ratio for the  $n = 0$  mode (simulated at 4.51 GHz and measured at 4.45 GHz on the azimuthal plane)



patterns of the two modes much, the geometry of the curved branches can be tuned to achieve CP for the  $n=0$  mode. The resonant frequency of  $n=0$  mode is determined approximately by the shunt resonance as  $f_0 = 1/(2\pi(L_L C_R)1/2)$ . Since the shunt capacitance can be increased by loading with curved branches which extend the current path, lower resonant frequency is achieved by longer branches.

The polarisation state can be found from the surface current distribution at four time points of  $t=0, T/4, T/2$  and  $3T/4$ , which is given in Fig. 4.  $T$  is the period of the charge and discharge states of the curved branches. Ninety degree phase difference

between the vertical and horizontal polarisation wave components is maintained corresponding to the time difference of  $T/4$ . Therefore CP omnidirectional patterns are realised for the dipole mode. The CP direction is determined by the direction of the curved branches. Right-hand CP (RHCP) characteristic is obtained for the proposed one because that the curved branches are directed to the counter-clockwise direction. When left-hand CP (LHCP) is needed, the curved branches should be arranged in the clockwise direction. Since the radiation patterns and polarisation property of the patch mode was not affected by the curved branches on the ground plane, the patch mode owns LP property.

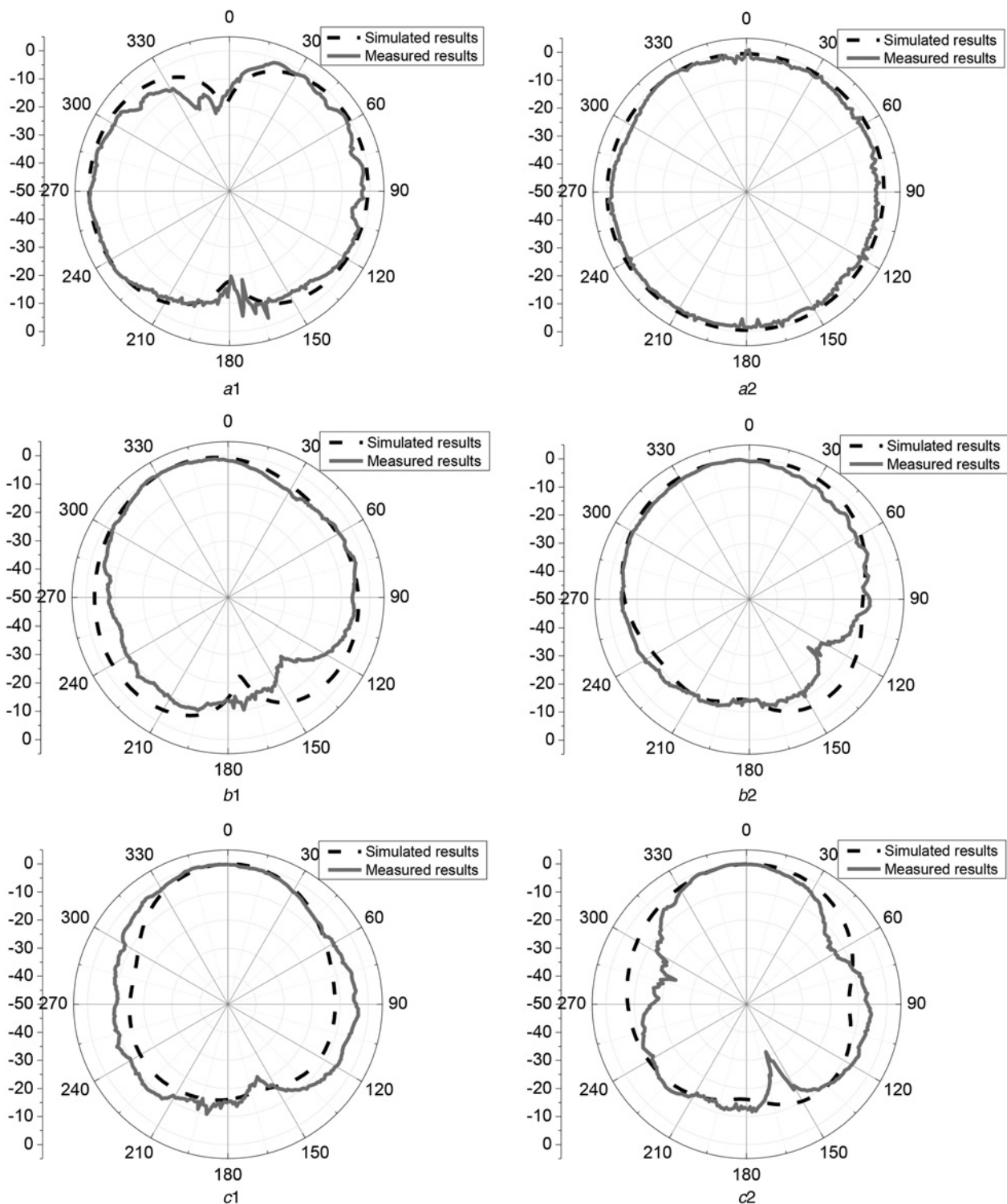


**Fig. 9** Simulated and measured radiation patterns of the proposed antenna at 4.45 GHz [a1:  $\phi = 45^\circ$  plane, a2:  $\theta = 90^\circ$  plane (XOY plane)], 5.6 GHz (b1:  $\phi = 45^\circ$  plane, b2:  $\phi = 135^\circ$  plane) and 5.9 GHz (c1:  $\phi = 45^\circ$  plane, c2:  $\phi = 135^\circ$  plane)

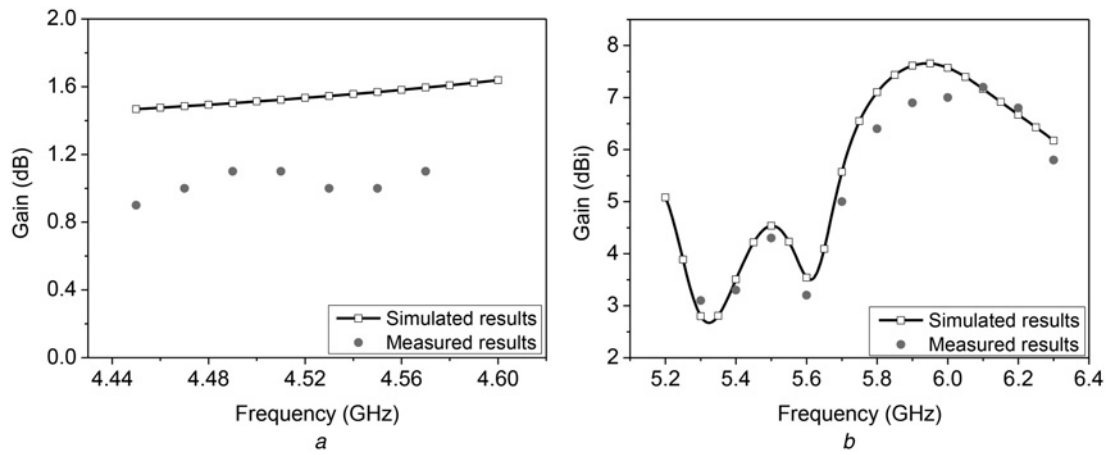


Fig. 10 Simulated and measured gain of the patch mode of the DBDMDP antenna

Table 2 Comparison between the former one and the proposed design

Type	Size	Bandwidth for the dipole mode	Bandwidth for the patch mode	Maximum gain for the dipole mode, dBi	Maximum gain for the patch mode, dBi	Numbers of substrate layers
one in [16]	100 × 100 × 2.5 (mm <sup>3</sup> )	2% (1.77 GHz)	1.9% (2.115 GHz)	1.2	5.4	2
proposed one	40 × 40 × 3 (mm <sup>3</sup> )	5.1% (4.42 GHz)	14.9% (5.74 GHz)	1.1	7.1	1

As shown in Fig. 5, the simulated axial ratio (AR) along azimuthal plane (the  $\theta=90^\circ$  plane) for the proposed antenna with various parameters ( $\beta_2$ ) or ( $\beta_3$ ) is described. It can be found that both the length and width of the curve strips plays important effect on the CP property. Thus the CP purity of the  $n=0$  mode can be optimised by tuning these parameters, and finally  $\beta_2=11^\circ$  and  $\beta_3=16^\circ$  are chosen. Fig. 5c shows the AR curves according to different frequencies. It confirms that the 3 dB AR bandwidth of the dipole mode is about 90 MHz from 4.49 to 4.58 GHz.

### 3 Results and discussion

A sample of the proposed antenna was fabricated to verify the antenna property, which is described in Fig. 6. The left and the right photographs show the top and bottom views, respectively. The proposed antenna is optimised by the HFSS software. The optimised parameters of the antennas are given in Table 1. The S-parameters were measured using an Agilent N5230A network analyser.

The measured reflection coefficients of the antenna are given in Fig. 7 and compared with the simulated results. Good agreement between the two can be obtained. It can be found that the measured  $-10$  dB return loss bandwidths is 5.1% (about 227.5 MHz) at the centre frequency of 4.42 GHz and 14.9% (857.5 MHz) at the centre frequency of 5.74 GHz for the dipole mode and patch mode, respectively. While the simulated  $-10$  dB return loss bandwidths of the two modes are 3.1 and 10%, respectively, the measured results of the modes are wider than the simulated ones. This may be due to the fabrication tolerances and the losses introduced by the dielectric and the SMA components.

As shown in Fig. 8, the AR of the antenna at the centre resonant frequency of the  $n=0$  mode is also measured and compared with the simulated results. The measured AR is  $<3.4$  dB in the azimuthal plane while the simulated AR is  $<3$  dB. Due to the four curved branches, four convexities exist at about  $\Psi=0^\circ, 90^\circ, 180^\circ$  and  $270^\circ$ , respectively. The results verify the CP properties of the omnidirectional mode.

As is shown in Fig. 9, measured radiation patterns were taken at 4.45, 5.6 and 5.9 GHz for both two planes, and compared with the

simulated ones. As shown in Figs. 9a1 and a2, a monopole like radiation pattern is achieved for the  $n=0$  mode (4.45 GHz). The gain variation is  $<3$  dB in the  $\theta=90^\circ$  plane (azimuthal plane) which is nearly omnidirectional with a null in the broadside direction. A peak gain of about 1.1 dBi is obtained for this mode. For  $n=+1$  mode (5.6 and 5.9 GHz), bore-sight radiation patterns with maximum gain nearly in the  $z$ -axial direction is obtained as predicted.

Finally, the axial direction gain against frequency for the patch mode of the antenna is measured and shown in Fig. 10. The maximum gain is about 7.1 dBi. Due to the soldering effect, metal and dielectric loss, the measured results are a little lower than the simulated ones. However, the agreement between the two is acceptable. What should be mentioned is that, gain drop occurs at the axial direction in the lower frequency band around 5.6 GHz. That is because the asymmetry probe-feeding structure contributes to the asymmetry radiation patterns at the lower band. The maximum beam direction is not right in the axial direction but tilted with a slope angle of about  $30^\circ$  in the  $\varphi=45^\circ$  plane. Both the measured and simulated patterns at 5.6 GHz shown in Figs. 9b1 and b2 confirm the analysis.

The DBDMDP antenna performance between the former design and the proposed one is given at Table 2. Both the two designs own unidirectional LP and omnidirectional CP characteristics. It can be found that the antenna bandwidth for both dipole mode and patch mode of the proposed design is much wider than the former design in [16]. Especially for the patch mode, the impedance bandwidth is about eight times wider than the former one. The maximum gain of the patch mode is also enhanced in the proposed design. Furthermore, with only one substrate layer, the proposed design owns much simpler structure, which is a good option for integration application.

### 4 Conclusion

Probe-feed single-layer DBDMDP patch antenna is proposed in this paper. Modified mushroom structure enables the dual-band dual-mode characteristic while curved branches employed in the ground plane excites the CP property for the  $n=0$  mode with

omnidirectional radiation patterns. Wide bandwidth is realised by loading with four curved patches around the circular radiating patch. Finally, one antenna prototype is fabricated to confirm the property. Moreover, the measured results shown that  $-10$  dB impedance bandwidths is 5.1 and 14.9% for the dipole mode and patch mode, respectively, which is much wider than former designs. This antenna concept is valuable in wireless communications with the advantages of simple structure, wide bandwidth, polarisation diversity and radiation pattern selectivity.

## 5 Acknowledgment

This work was supported by the National Science Foundation of China under grant 61401506.

## 6 References

- 1 James, J.R., Hall, P.S. (Eds): 'Handbook of microstrip antenna' (Peter Peregrinus, London, UK, 1989), vol. 1
- 2 Nunes, R., Moleiro, A., Rosa, J., *et al.*: 'Dual-band microstrip patch antenna element with shorting pins for GSM'. IEEE Antennas and Propagation Society Int. Symp., July 2000, vol. 2, pp. 16–21
- 3 Wong, K.-L., Chiou, T.-W.: 'Broad-band dual-polarized patch antennas fed by capacitively coupled feed and slot-coupled feed', *IEEE Trans. Antennas Propag.*, 2002, **50**, (3), pp. 346–351
- 4 Chen, Q., Kurahashi, M., Sawaya, K.: 'Dual-mode patch antenna with pin diode switch'. 6th International Symposium Antennas, Propagation and EM Theory Proc., November 2003, pp. 66–69
- 5 Chiu, C.Y., Murch, R.D.: 'Compact four-port antenna suitable for portable MIMO devices', *IEEE Antennas Wirel. Propag. Lett.*, 2008, **7**, pp. 142–144
- 6 Sim, C.-Y.-D., Chang, C.-C., Row, J.-S.: 'Dual-feed dual-polarized patch antenna with low cross-polarization and high isolation', *IEEE Trans. Antennas Propag.*, 2009, **57**, (10), pp. 3321–3324
- 7 White, C.R., Rebeiz, G.M.: 'A differential dual-polarized cavity-backed microstrip patch antenna with independent frequency tuning', *IEEE Trans. Antennas Propag.*, 2010, **58**, (11), pp. 477–487
- 8 Hong, Y.-P., Kim, J.-M., Jeong, S.-C., *et al.*: 'Low-profile S-band dual-polarized antenna for SDARS application', *IEEE Antennas Wirel. Propag. Lett.*, 2005, **4**, pp. 475–477
- 9 Afshinmanesh, F., Marandi, A., Shahabadi, M.: 'Design of a single-feed dual-band dual-polarized printed microstrip antenna using a Boolean particle swarm optimization', *IEEE Trans. Antennas Propag.*, 2008, **56**, (7), pp. 1845–1852
- 10 Sievenpiper, D., Zhang, L., Broas, R.F.J., *et al.*: 'High-impedance electromagnetic surfaces with a forbidden frequency', *IEEE Trans. Microw. Theory Tech.*, 1999, **47**, (11), pp. 2059–2074
- 11 Caloz, C., Itoh, T.: 'Electromagnetic metamaterials: transmission line theory and microwave applications' (Wiley-IEEE Press, Hoboken-Piscataway, 2005)
- 12 Cao, W.Q., Zhang, B.N., Yu, T.B., *et al.*: 'Single-feed dual-band dual-mode and dual-polarized microstrip antenna based on metamaterial structure', *J. Electromagn. Waves Appl.*, 2011, **25**, (13), pp. 1909–1919
- 13 Cao, W.Q., Zhang, B.N., Liu, A.J., *et al.*: 'Multi-frequency and dual-mode patch antenna based on electromagnetic band-gap (EBG) structure', *IEEE Trans. Antennas Propag.*, 2012, **60**, pp. 6007–6012
- 14 Park, B.C., Lee, J.H.: 'Omnidirectional circularly polarized antenna base on meta material transmission line'. *IEEE AP-S*, June 2009
- 15 Park, B.-C., Lee, J.-H.: 'Omnidirectional circularly polarized antenna utilizing zeroth-order resonance of epsilon negative transmission line', *IEEE Trans. Antennas Propag.*, 2008, **56**, (7), pp. 1845–1852
- 16 Cao, W.Q., Zhang, B.N., Liu, A.J., *et al.*: 'A dual-band microstrip antenna with omnidirectional circularly polarized and unidirectional linearly polarized characteristics based on metamaterial structure', *J. Electromagn. Waves Appl.*, 2012, **26**, (2–3), pp. 274–283
- 17 Cao, W.Q., Liu, A.J., Zhang, B.N., *et al.*: 'Multi-band multi-mode microstrip circular patch antenna loaded with metamaterial structures', *J. Electromagn. Waves Appl.*, 2012, **26**, (7), pp. 923–931
- 18 Cao, W.Q., Liu, A.J., Zhang, B.N., *et al.*: 'Dual-band spiral patch-slot antenna with omnidirectional CP and unidirectional CP properties', *IEEE Trans. Antennas Propag.*, 2013, **61**, pp. 2286–2289
- 19 Cao, W.Q., Zhang, B.N., Liu, A.J., *et al.*: 'Microstrip antenna with radiation pattern selectivity and polarized diversity based on modified metamaterial structure'. 2012 Int. Conf. on Microwave and Millimeter Wave Technology (ICMMT), 2012
- 20 Cao, W.Q., Zhang, B.N., Liu, A.J., *et al.*: 'A reconfigurable microstrip antenna with radiation pattern selectivity and polarization diversity', *IEEE Antennas Wirel. Propag. Lett.*, 2012, **11**, pp. 453–456
- 21 Cao, W.Q., Zhang, B.N., Liu, A.J., *et al.*: 'Novel phase-shifting characteristic of CRLH TL and its application in the design of dual-band dual-mode dual-polarization antenna', *Prog. Electromagn. Res.*, 2012, **131**, pp. 375–390

Copyright of IET Microwaves, Antennas & Propagation is the property of Institution of Engineering & Technology and its content may not be copied or emailed to multiple sites or posted to a listserv without the copyright holder's express written permission. However, users may print, download, or email articles for individual use.